Radiology Case Reports 19 (2024) 2590–2595

Available online at www.sciencedirect.com

ScienceDirect

journal homepage: www.elsevier.com/locate/radcr

Case Report

Erdheim-Chester Disease presenting with constrictive pericarditis: A case report and review of the literature ☆,☆☆

Ge Guo, MD[a], *Danfeng Zheng, MD*[b], *Xiaohua Wang, MD*[a], *Xinyu Wang, MD*[c,*]

[a] *Department of Radiology, Peking University Third Hospital, Beijing, 100191, China*
[b] *Department of Pathology, Peking University Third Hospital, Beijing, 100191, China*
[c] *Department of Cardiology and Institute of Vascular Medicine, Peking University Third Hospital; State Key Laboratory of Vascular Homeostasis and Remodeling, Peking University; NHC Key Laboratory of Cardiovascular Molecular Biology and Regulatory Peptides, Peking University; Beijing Key Laboratory of Cardiovascular Receptors Research. Beijing, China*

ARTICLE INFO

Article history:
Received 18 December 2023
Revised 23 February 2024
Accepted 26 February 2024

Keywords:
Erdheim-Chester Disease
Constrictive pericarditis
Histiocytosis
Multisystemic involvement
Imaging modalities
Interferon-α2b

ABSTRACT

Erdheim-Chester Disease (ECD) is a rare form of histiocytosis characterized by xanthomatous infiltration of affected organs. We present a case of a 62-year-old man with ECD initially presenting with constrictive pericarditis. Comprehensive imaging revealed systemic involvement, including the skeleton, orbit, pituitary, lung, kidney, and retroperitoneum, despite the absence of related symptoms. The diagnosis of ECD was eventually confirmed through histopathological evidence from a CT-guided biopsy. The patient responded well to interferon-α2b treatment, with gradual symptom amelioration and improvement in imaging and laboratory findings over a 5-month follow-up period. This case highlights the importance of considering ECD in the differential diagnosis of constrictive pericarditis and the utility of multimodal imaging for accurate diagnosis and management of this rare disease. The patient's positive response to treatment also highlights the potential for effective management of ECD, particularly with early diagnosis and intervention.

☆ Acknowledgments: Julian Heng (Remotely Consulting, Australia) provided professional English-language editing of this article (Manuscript Certificate No. 6Dl7Bu3W). This work was supported by the Haidian Innovation Transformation Fund of China (HDCXZHKC2021216).

☆☆ Competing Interests: The authors declare that they have no known competing financial interests or personal relationships that could have appeared to influence the work reported in this paper.

* Corresponding author.
E-mail address: saplingwxyw@hotmail.com (X. Wang).

https://doi.org/10.1016/j.radcr.2024.02.087

Background

Erdheim-Chester disease (ECD) is a rare, non-inherited, non-Langerhans form of histiocytosis with multisystemic manifestations. Since it was first described by Jakob Erdheim and William Chester in 1930, more than 1000 cases of ECD have been reported, predominantly in individuals 40 to 70 years of age with a slight predominance in males [1]. ECD is characterized by xanthomatous infiltration of the affected organs by foamy histiocytes which immunostain for CD68 but not for CD1a. The proto-oncogene BRAF V600E is mutated in 38%-68% of ECD cases [2].

ECD can manifest with a wide spectrum of symptoms, ranging from virtually asymptomatic to a multi-systemic presentation. The most common manifestation is bone pain, which appears in over 50% of patients [3]. Moreover, approximately half of documented ECD patients also experience extra-skeletal manifestations, largely affecting the central nervous system, orbital region, renal system, retroperitoneal area, cardiovascular system, and respiratory system.

For some cases with cardiovascular issues, pericardial involvement can result in pericarditis, effusion, and even tamponade [4–6]. Here, we describe a rare case initially presenting as constrictive pericarditis without symptoms of other affected systems. This particular clinical scenario posed a diagnostic challenge before a multidisciplinary approach was applied to accurately diagnose and treat ECD symptoms.

Case presentation

A 62-year-old man of Chinese origin was referred to the Department of Cardiology (Peking University Third Hospital) with cough, expectoration, dyspnea, edema of lower extremities. He also claimed reduced appetite for 2 months and was found to have lost 5 kg of body weight in the last month. He had a history of coronary artery disease and carotid artery stenosis. Physical examination showed tachycardia, jugular venous distension without liver jugular reflux sign or Kussmaul's sign, and symmetrical concave edema in lower extremities.

An initial laboratory investigation revealed elevated N-terminal pro-B-type natriuretic peptide (NT-proBNP) (4051 pg/mL, normal<125 pg/mL) and C-reactive protein (7.89 mg/dL, normal<0.8 mg/dL). The routine blood test, liver function and renal profile were normal. Electrocardiogram was remarkable for sinus tachycardia, low voltage of limb leads, and T-wave changes.

A transthoracic echocardiogram (TTE) demonstrated remarkable thickening of pericardium of up to 9.4 mm without pericardial effusion, typical ventricular septal bounce, enlargement of left atrium, reduced left ventricular ejection fraction (LVEF 42%), decreased LV diastolic function, and inferior vena cava plethora with low inspiratory collapse. A cardiac contrast-enhanced computed tomography (CT) scan revealed thickening of the pericardium without calcification, dilated aorta with thickening of the wall involving its branches, and soft tissue infiltration in pericardium cavity with slightly enhancement which sheathed the right and left coronary arteries (Fig. 1). Cardiovascular magnetic resonance imaging (CMR) demonstrated diffuse thickening of pericardium and aortic wall with remarkable late gadolinium enhancement (LGE), enlargement of left and right atrium (RA), ventricular septal bounce, decreased LVEF (40%), and inferior vena cava plethora (Fig. 2).

Taken together, observations from the TTE, CT and CMR data were consistent with constrictive pericarditis (CP). CP has a wide range of differential diagnosis including tuberculosis, idiopathic, infection, malignancy, collagen vascular disease, trauma, or related to prior cardiac surgery and chest irradiation [7]. Yet, the patient did not have a history of trauma, surgery or tumor growth. Furthermore, all tests carried out which were related to infections including tuberculosis were negative, as well as available serum tumor markers, autoimmune antibodies and serum levels of IgG subclass.

Further examination including chest CT revealed thickening of interlobular septa in the lower lobes and bilateral pleural effusion (Fig. 3A). Abdominal CT showed bilateral perirenal soft tissue halo involving renal pelvis causing mild bilateral hydronephrosis (Fig. 3B), thickening of abdominal aortic wall, bilateral adrenal glands and peritoneum. MRI of pituitary gland suggested enlarged pituitary with disappearance of neurohypophysis hyperintensity on T1-weighted imaging, and thickening of the tentorium cerebellum (Fig. 3C). However, there was no evidence of endocrinopathy (pituitary, adrenal and thyroid functions) in laboratory studies. Orbital enhanced magnetic resonance imaging (MRI) showed bilateral orbital soft tissue masses with enhancement (Fig. 3D).

We conducted ^{18}F-flourodeoxyglucose (^{18}F-FDG) positron emission tomography (PET) imaging and detected relatively abnormal uptake and thickening of multiple foci throughout the body (Fig. 3E-H), including tentorium cerebelli, bilateral orbital soft tissue, pericardium, periaortic soft tissue, pleura, renal capsule, bilateral adrenal glands, parietal peritoneum and left testis. These radiological images narrowed the differential diagnosis to lymphoma, histiocytosis or IgG4-related disease (IgG4-RD).

The case was forwarded to a multidisciplinary team meeting (MDT) and a possible diagnosis of ECD was made by the radiologist. ^{99m}Tc-Methylenediphosphonate (^{99m}Tc-MDP) bone scintigraphy (Fig. 4A) suggested hyperactivity of bilateral distal femurs, with both ends of tibias and the left humeral head, which was consistent with ECD. A CT-guided biopsy was obtained from the right proximal tibia. Histopathologic findings showed diffuse infiltration by foamy histiocytes that immunostaining for CD68 (+), S-100 (partial +), CD163 (+), FXIIIA (+), and Lysozyme (+), but CD1a (-), Langerin (-) and BRAF V600E (-); altogether consistent with ECD histopathological diagnosis (Fig. 5). Genetic study showed no mutation of BRAF gene Exon-15(V600E) (data not shown).

The patient was referred to hematology department and interferon-α2b (IFN-α2b) was administered at a dose of 3 million units (mIU), 3 times per week. The patient suffered fever after the first injection, which subsided spontaneously within a few hours. Over the course of a 5-month follow-up period, the patient's symptoms exhibited gradual amelioration, concomitant with a reduction in serum NT-proBNP levels to

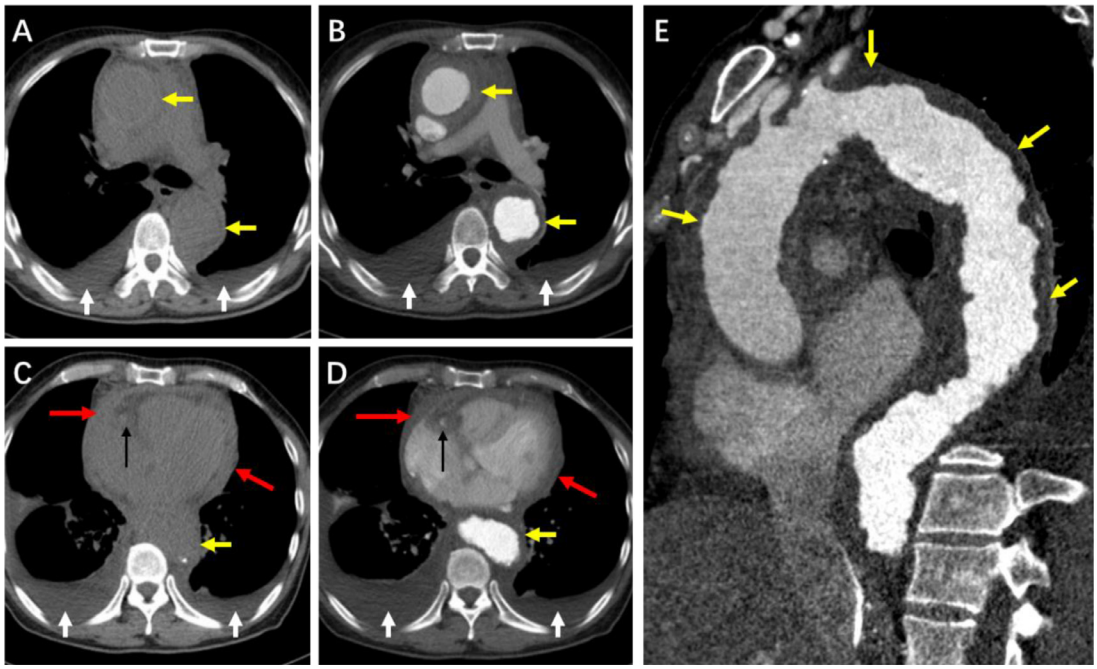

Fig. 1 – Cardiac computed tomography (CT) scan. (A, C) Axial non-enhanced CT. (B, D) Axial contrast-enhanced CT. Axial images revealed thickening of the pericardium (red arrows), dilated aorta with wall thickening (yellow arrows) and soft tissue infiltration in pericardium cavity which sheathed the right (black arrows) and left coronary arteries. Bilateral pleural effusions were also presented (white arrows). (E) Sagittal enhanced image showed evidence of a coated aorta (yellow arrows).

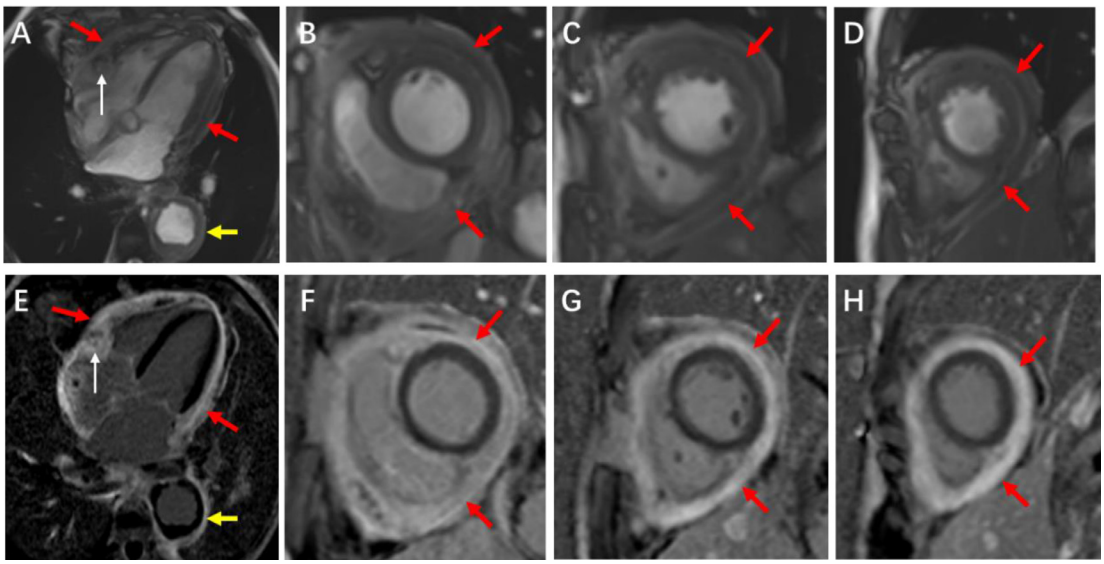

Fig. 2 – Cardiac magnetic resonance (CMR) imaging. Balanced Steady-state free precession (b-SSFP) of four-chamber (A) and short axis (B-D) views at end-diastolic phase of left ventricle showed diffuse thickening of pericardium (red arrows) and aortic wall (yellow arrow), with soft tissue infiltration encasing right coronary artery (white arrow). Late gadolinium enhancement (LGE) images of the same location (E-H) showed remarkable LGE of thickened pericardium (red arrows), aortic wall (yellow arrow) and soft tissue of right atrioventricular groove (white arrow).

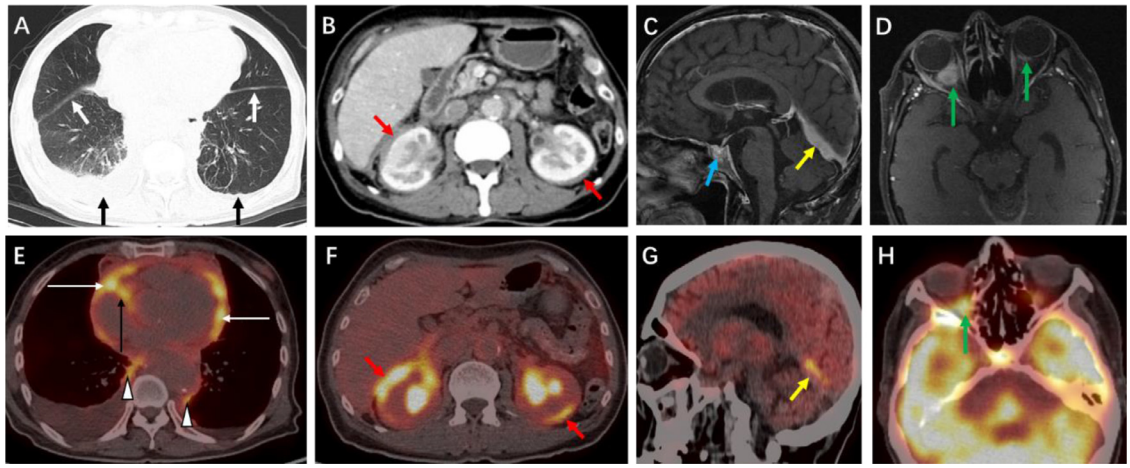

Fig. 3 – (A) Chest CT revealed thickening of interlobular septa in the lower lobes, fissural thickening (short white arrows) and bilateral pleural effusions (short black arrows). (B) Abdominal enhanced CT showed bilateral perirenal soft tissue halo (hairy kidney) (red arrows), involving renal pelvis causing bilateral hydronephrosis. (C) Enhanced magnetic resonance imaging (MRI) of pituitary gland suggested enlarged pituitary with heterogeneous enhancement (blue arrow), thickening and enhancement of the tentorium cerebellum (yellow arrow). (D) Orbital enhanced MRI showed bilateral orbital soft tissue masses with enhancement (green arrows). (E-H) ^{18}F-flourodeoxyglucose (^{18}F-FDG) positron emission tomography (PET) imaging showed relatively avid uptake of FDG in thickened pericardium (long white arrow), soft tissue of right atrioventricular groove (long black arrow), periaortic soft tissue, bilateral pleura (arrowheads), renal capsule (red arrows), tentorium cerebelli (yellow arrow) and orbital soft tissue (green arrow).

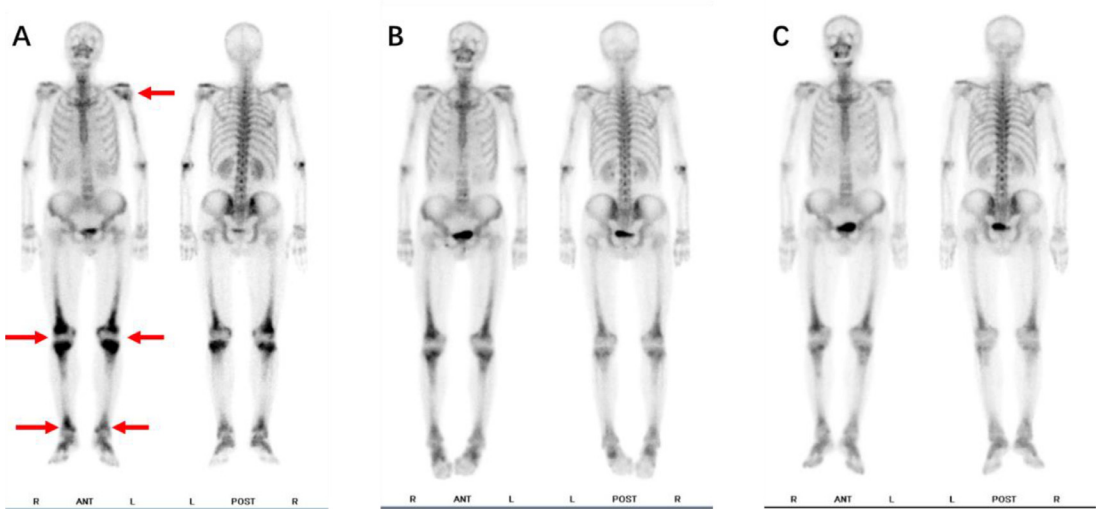

Fig. 4 – (A) ^{99m}Tc-Methylenediphosphonate (^{99m}Tc-MDP) bone scintigraphy suggested hyperactivity of bilateral distal femurs, both ends of tibias and left humeral head (red arrows). (B) Repeat bone scintigraphy conducted 2-months after treatment. (C) Repeat bone scintigraphy conducted 5-months after treatment. Repeat images showed a progressive decrease in metabolism of the femur, tibia, and left humeral head.

within the normal range. Repeat bone scintigraphy conducted at 2-months (Fig. 4B) and 5-months (Fig. 4C) after treatment revealed a progressive diminution in metabolic activity within the femur, tibia, and left humeral head. Furthermore, the volume of orbital soft tissue masses displayed a decrement, TTE exhibited a reduction in pericardial thickness along with restoration of normal LVEF.

Discussion

The most common manifestations of ECD include bone pain, diabetes insipidus and exophthalmos [8,9]. In this case, we described an ECD patient initially presenting with CP, which is rarely reported in the literature. Interestingly, this patient fea-

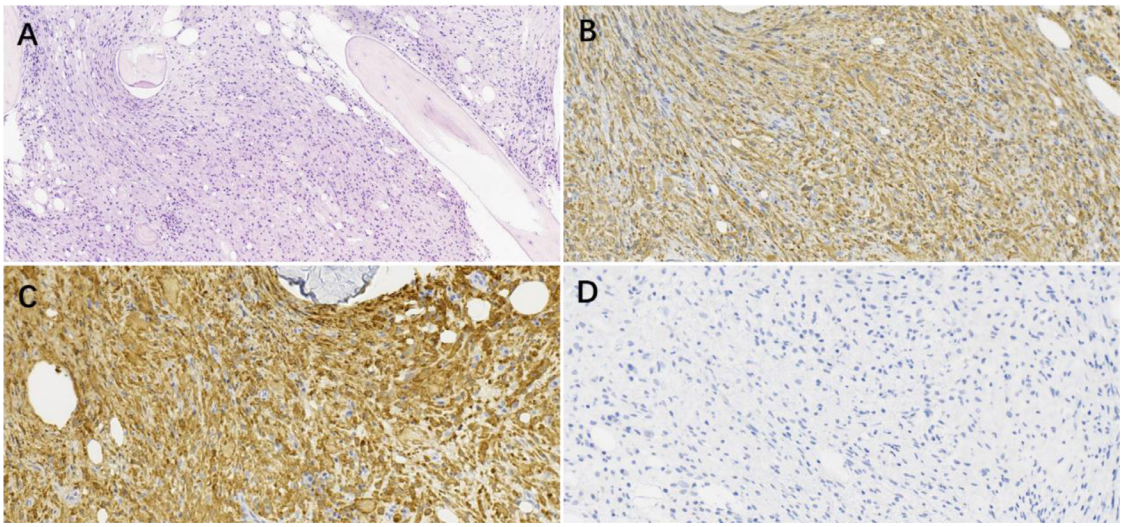

Fig. 5 – Histopathological findings from a bone marrow biopsy obtained from the right proximal tibia. (A) Micrographs of Hematoxylin-eosin-stained sections (20x magnification) showed infiltration of histiocytes with single small nuclei and foamy cytoplasm. Touton cells were also observed. (B-D) Immunohistochemistry staining (40x magnification) showed that histiocytes were positive for CD68 (B) and CD163 (C), and negative for Langerin (CD207) (D).

tured multisystemic involvement including skeleton, orbit, pituitary, lung, kidney and retroperitoneum, but relevant symptoms were absent. Multimodal imaging modalities showed some typical radiological features of ECD, which helped steer the eventual diagnosis of the patient.

Although frequently asymptomatic for cardiovascular issues, such involvement does occur in two-thirds of ECD patients with poor prognosis and are typically detected incidentally on radiological imaging, including peri-adventitial infiltration of aorta (coated aorta), valvular disease, pseudotumoural infiltration of the chambers of the right side of the heart, and pericardial disease. Other causes of similar systemic diseases, such as IgG4-related disease (IgG4-RD), should be considered as differential diagnoses [10]. The cardiovascular involvement of IgG4-RD includes aortitis or inflammatory aneurysms of large-to-middle-size vessels, stenosis or aneurysm and diffuse wall thickening of coronary arteries (pigs-in-a-blanket sign), myocardial infiltration, and pericarditis [11]. Evaluation of serum IgG4 concentration and histopathological investigation may contribute to the differential diagnosis.

Pericardial involvement occurs in 29% of ECD patients [1], and characterized by abnormal thickening, effusions, or cardiac tamponade [12]. In this case, the most prominent clinical finding was CP, which always poses a challenging diagnostic path. Tuberculosis remains a dominant cause of CP in China, with the next most dominant causes being idiopathic pericarditis, infection, malignancy, systemic autoimmune disease, trauma, or history of cardiac surgery and chest irradiation. For our patient in this case study, the serological test, sputum tests and chest CT did not support the diagnosis of tuberculosis. The presence of significant weight loss prompted a mandatory examination for potential neoplastic or systemic autoimmune disease. But the hypothesis of an autoimmune disease was less likely due to the sex and age of the patient, and the absence of serological markers tested. The search for a neoplastic disease began with the serum tumor markers, followed by the whole-body imaging examinations, which then sufficiently raised suspicion for less common entities in clinical practice.

Typical CT findings of ECD include the “coated aorta” and “hairy kidneys”, due to the infiltration of perirenal fat. Bone scintigraphy showed intense uptake at the end of long bones, which is reported in 80%-96% of ECD patients. As in this case, the biopsy is usually the confirmatory examination, showing infiltrating CD68+, CD1a- foamy histiocytes.

The comprehensive baseline assessment is very important to characterize the burden of disease before treatment of ECD, and the use of repeat PET-CT or bone scintigraphy scans are sensitive for assessing ECD activity and therapeutic responses. Although CNS and cardiovascular involvement, which were both present in this case, are predictors of poor prognosis [8], our patient showed good response to IFN-α2b treatment. The curative effects may also have been attributable to a relatively early diagnosis and treatment for our patient. Close long-term follow-up will be required to evaluate the efficacy of the treatment and to understand the on-going prognosis of this patient.

Conclusion

ECD, though a rare cause of CP, should be considered in a differential diagnosis scenario, as in this case. When pericardium involvement is associated with periaortic tissue infiltration, the diagnosis of ECD should be raised to a search for the other diagnostic criteria of the disease, such as bone involvement or perirenal infiltration and histological confirmation. Multimodal imaging modalities were necessary to comprehen-

sively evaluate the involvement of different organs. Recognition of characteristic imaging features of ECD will help prompt and correctly diagnose this rare condition.

Patient consent

Our institution does not require ethics approval for reporting individual cases or case series. Informed consent for publication of the case was obtained from the patient. All patient identifying information has been removed in writing this case report.

REFERENCES

[1] Haroche J, Cohen-Aubart F, Amoura Z. Erdheim-Chester disease. Blood 2020;135(16):1311–18.
[2] Diamond EL, Dagna L, Hyman DM, et al. Consensus guidelines for the diagnosis and clinical management of Erdheim-Chester disease. Blood 2014;124(4):483–92.
[3] Merai H, Collas D, Bhagat A, Mandalia U. Erdheim-Chester disease: a case report and review of the literature. J Clin Imaging Sci 2020;10:37.
[4] Nicolazzi MA, Carnicelli A, Fuorlo M, Favuzzi AMR, Landolfi R. Cardiovascular involvement in Erdheim-Chester disease: a case report and review of the literature. Medicine (Baltimore) 2015;94(43):e1365.
[5] Das JP, Xie L, Riedl CC, Hayes SA, Ginsberg MS, Halpenny DF. Cardiothoracic manifestations of Erdheim-Chester disease. Br J Radiol 2019;92(1104):20190473.
[6] Yoon M, Lee SH, Shim HS, Kang SM. Erdheim-Chester disease presenting as an intracardiac mass and pericardial effusion confirmed by biopsy: a case report. Eur Heart J Case Rep 2021;5(10):ytab351.
[7] Welch Terrence D. Constrictive pericarditis: diagnosis, management and clinical outcomes. Heart 2018;104(9):725–31.
[8] Mishra AK, Mani S, George AA, Sudarsanam TD. Recurrent pericardial effusion and tamponade in a patient with Erdheim-Chester disease (ECD). BMJ Case Rep 2015;2015 bcr2015212483.
[9] Kumar P, Singh A, Gamanagatti S, Kumar S, Chandrashekhara SH. Imaging findings in Erdheim-Chester disease: what every radiologist needs to know. Pol J Radiol 2018;83:e54–62.
[10] Lanzafame LRM, Carerj ML, Rizzo G, Minutoli F, Bucolo GM, Irrera N, et al. Multimodality imaging evaluation of coronary IgG4-related disease: a “tumor-like” cardiac lesion. Diagnostics (Basel) 2022;12(11):2814.
[11] Chandrashekhara SH, Ojha V, Kumar P, Goyal A, Kumar S. IgG4-related cardiovascular disease: imaging features on cardiac computed tomography and magnetic resonance imaging. Indian J Thorac Cardiovasc Surg 2022;38(4):451–3.
[12] Oliveira M, Monteiro S, Dos Santos J, Silva AC, Morais Ferreira R. Erdheim-Chester disease: a rare clinical entity. Eur J Case Rep Intern Med 2020;7(9):001630.